Formation of Superlattice in Face-Centered Cudic Lattice with a Special Reference to the Copper-Platinum System

Formation of Superlattice in Face-Centered Cudic Lattice with a Special Reference to the Copper-Platinum System*

Tokutaro HIRONE and Kengo ADACHI

The Research Institute for Iron, Steel and Other Metals

(Received March 9, 1955)

Synopsis

Based on the notion that, for the formation of certain types of superlattices in face-centered cubic alloys, the second neighbor interaction becomes appreciable, the formation of superlattice in copper-platinum system was studied, and the ordering energy in such a formation was obtained from the viewpoint of electron theory. The results could interpret both quantitatively and qualitatively various results of many experiments concerning this binary system.

I. Introduction

Among the superlattices in binary or ternary systems, there are some cases, in which they are formed by the interactions between the pair of nearest neighboring atoms and those between the second and farther neighbors, such as in the cases of Fe_3Al, CuPt and Heusler alloys(1). Based on this fact, the present authors have reported the study of the formation of various superlattices of body-centered cubic binary alloys. In the present paper, an attempt will be shown to solve the problem of the formation of superlattices of various types in face-centered cubic binary alloys from the same point of view as before.

According to Mott(2), the so-called ordering energy, $V=\frac{1}{2}(V_{AA}+V_{BB})-V_{AB}$, in the statistical theory of the superlattice of two kinds of metallic atoms A and B, is presumed to be composed of two terms of energy. One is due to the difference between the exchange repulsions of like and unlike atoms and the other is based on the electrostatic energy of rather ionic nature between the screened polar atoms in the metals. The former comes into consideration in respect of the nearest neighbor atoms, but the latter extends to atoms farther than the nearest neighbor. Consequently, in the alloy systems wherein the latter energy is large, the interaction between the pair of second neighbor or farther atoms may become signifi cant, leading to the formation of superlattices as found in Fe_3Al and CuPt. If, however, only the reasons introduced by Mott are taken into consideration, it follows that superlattices should be found almost in all cases of solid solutions of metals with unequal valences, but this is not the case.

As another important factor for the formation of superlattice, the splitting of

* The 798th report of the Research Institute for Iron, Steel and Other Metals.

(1) K. Adachi, Sci. Rep. Tôhoku Univ, (I) **35** (1951), 30.
S. Matsuda, J. Phys. Soc. Japan, **6** (1951), 151; **8** (1953), 20.
H. K. Hardy, Sci. Rep. Tôhoku Univ., (I) **36** (1952), 156.
(2) N. F. Mott, Proc. Phys. Soc., **49** (1937), 258.

Brillouin zones may be taken up, when based on the energy band theory of alloys[3]. For example, when Hall constant[4] is considered in the superlattice of the alloy of monovalent metals, Cu_3Au, the influence of such a splitting appears to be essential. Especially, when the Fermi surface and the boundary surface of the new Brillouin zones generated by the band splitting are closely situated, this influence becomes predominant. Recently, Nicholas[5] has discussed the ordering energy of superlattices in stoichiometric composition of CuAu, CuPt etc. On the basis of the Brillouin zone theory, however, no convincing conclusion arrived at before the thoroughgoing study of the electronic structure of alloys was achieved. From the viewpoint of electron theory of metallic alloys, the ordering energy pointed out by Mott and that deduced from the Brillouin zone effect cannot be mutually unrelated. Without entering into detailed discussion concerning the Brillouin zone effect, a unified discussion on the formation of superlattices in facecentered cubic systems will be shown below, especially of the various types of superlattices in Cu-Pt system, based on Mott's discussion and taking the interactions between the nearest as well as the second neighbor into consideration.

II. Formation of superlattice in face-centered cubic crystal

1. Definition of order parameters

For simplicity, the ordering in atomic arrangement will first be formulated in the case of larger unit cell than the original one, taking into account the interaction between the pair of atoms farther than the second neighbors. Let N and N_ν be the total numbers of the lattice points and the sublattice points, respectively, and P_i^ν the occupation probability of i-th atoms on ν-th sublattice. The latter corresponds to the degree of long range order. Then, the energy U and entropy Φ of the total system will be given as follows:

$$U = \frac{N}{2} z^\xi \sum_\xi \sum_{i,j} \sum_{\mu,\nu} V_{ij}^\xi P_i^\nu P_j^\mu , \tag{1}$$

$$\Phi = k \ln \left[\prod_i \prod_\nu (N_\nu!) \Big/ (P_i^\nu N_\nu!) \right], \tag{2}$$

where ξ is a notation showing the neighboring index, z^ξ is the coordination number of the ξ-th neighbors. The equilibrium value of P_i^ν under finite temperature may be determined by solving simultaneously the equations $\partial F/\partial P_i^\nu = 0$, which are the equilibrium conditions of the free energy $F = U - T\Phi$ with respect to the variables P_i^ν. Since the conditions $\sum_\nu P_i^\nu = (N/N_\nu) x_i$ and $\sum_i P_i^\nu = 1$ (where x_i is the concentration of the i-th elements) hold between the variables P_i^ν, the number of independent variables will be reduced to $(i-1)\times(\nu-1)$.

(3) T. Muto, Sci. Pap. Inst. Phys. Chem. Res., Tokyo, **34** (1938), 377; J.C. Slater, Phys. Rev., **84** (1951), 179.

(4) Komar and Sidorov, J. Tech. Phys. U.S.S.R., **11** (1941), 711; J. Phys. U.S.S.R., **4** (1941), 552.

(5) N. F. Nicholas, Proc. Phys. Soc., A**66** (1953), 201.

2. Superlattices of various types in Cu-Pt system

When the second neighbor interaction is to be taken into account in face-centered cubic type superlattice, the cell with twice the original lattice constant must be taken as the unit one, which may be formed by the interpenetration of 8 f. c. c. sublattices, α_1, α_2, $\cdots$ δ_2, with the double lattice constant (Fig. 1). Then, in binary alloys of f. c. c. type, 9 types of superlattices can be considered as shown in Table 1. The atomic occupation in the superlattices of the different types may be inferred from the values of α's shown in the fourth column of the table. For convenience's sake, those different types are designated by the notations in the brackets in the second column. According to the definition given above, $i=2$ and $\nu=8$, and so the independent variables in P_i^ν become 7, resulting in 7 simultaneous equations of equilibrium conditions of the free energy of this system. As it was very complicated to solve these 7 equations in a general manner, the free energy in general cases was first calculated and then the simultaneous equations were solved in each case given in Table 1.(*)

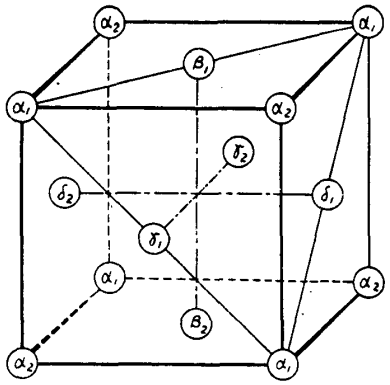

Fig. 1. Sublattices in *f.c.c.* crystal.

Table 1. Various types of superlattice in f. c. c. binary alloy.

Types of superlattice	Notation	Range of x(*)	Occupation probability (ord.~disord.)	Energy at 0°K
Perfect Disord	[O]	$0 \leqq x \leqq 1$	x	$4(6+\mu)x^2$
CuAu type	[I_0]	$0 \leqq x \leqq 1/2$	α, $(2x \sim x)$	$4(4+2\mu)x^2$
Cu_3Au type	[I_1]	$0 \leqq x \leqq 1/4$,	α, $(4x \sim x)$; β, $(0 \sim x)$	$16\mu x^2$
		$1/4 \leqq x \leqq 1/2$	α, $(1 \sim x)$; β, $(4x-1 \sim x)$	$2(2-\mu)(4x-1)+16\mu x^2$
	[I_2]	$1/4 \leqq x \leqq 1$	α, $(1 \sim x)$	$\frac{4}{3}(2+\mu)(1-2x)(4x-1)+16\mu x^2$
CuPt type	[II_0]	$0 \leqq x \leqq 1/2$	a, $(0 \sim x)$	$24x^2$
$CuPt_7$	[II_1]	$0 \leqq x \leqq 1/8$	a, $(0 \sim x)$; b, $(8x \sim x)$	0
$CuPt_3$	[II_2]	$1/8 \leqq x \leqq 1/4$	a, $(0 \sim x)$; , $(1 \sim x)$; c, $(8x-1 \sim x)$	$8x-1$
Cu_3Pt_5	[II_3]	$1/4 \leqq x \leqq 3/8$	a, $(0 \sim x)$; , $(1 \sim x)$; c, $(8x-2 \sim x)$	$16x-3$
	[II_4]	$3/8 \leqq x \leqq 1/2$	a, $(0 \sim x)$; b, $(1 \sim x)$	$6(4x-1)$

(*) The same can be said for the concentration of another element, $1-x$.

*) Here we tetatively treat the system as if it were of a perfect face-centered cubic lattice, neglecting the fact that the CuAu type and CuPt type crystals have slightly tetragonal or rhombohedral structure.

For simplicity P^{ν}_{Cu} be α_1 etc., the concentration x_{Cu} be x and the ratio of the nearest and second neighbor interaction be μ. Thus,

$$\mu = \frac{2nd.\ neigh.\ interact.}{1st.\ neigh.\ interact.} = \frac{z_{II}}{z_I} \cdot \frac{W_{AA}+W_{BB}-2W_{AB}}{V_{AA}+V_{BB}-2V_{AB}} = \frac{1}{2}\frac{W}{V}. \tag{3}$$

Now, representing the temperature scale with $\theta = \frac{2kT}{z_I V}\left(\frac{N}{N_\nu}\right) = \frac{4}{3}kT$, the free energy, $f = 2F/z_I NV$ was calculating from (1) and (2):

$$\begin{aligned} f = &-\Big[(\alpha_1+\alpha_2)^2+(\beta_1+\beta_2)^2+(\gamma_1+\gamma_2)^2+(\alpha_1+\alpha_2)(\beta_1+\beta_2)+(\beta_1+\beta_2)(\gamma_1+\gamma_2) \\ &\quad +(\gamma_1+\gamma_2)(\alpha_1+\alpha_2)-8x(\alpha_1+\alpha_2+\beta_1+\beta_2+\gamma_1+\gamma_2)\Big] \\ &+\mu[\alpha_1\alpha_2+\beta_1\beta_2+\gamma_1\gamma_2+\delta_1\{8x-(\alpha_1+\alpha_2+\beta_1+\beta_2+\gamma_1+\gamma_2+\delta_1)\}] \\ &+\theta\Big[\alpha_1\ln\alpha_1+(1-\alpha_1)\ln(1-\alpha_1)+\beta_1\ln\beta_1+(1-\beta_1)\ln(1-\beta_1)+\gamma_1\ln\gamma_1 \\ &\quad +(1-\gamma_1)\ln(1-\gamma_1)+\delta_1\ln\delta_1+(1-\delta_1)\ln(1-\delta_1)+\alpha_2\ln\alpha_2+(1-\alpha_2)\ln(1-\alpha_2) \\ &\quad +\beta_2\ln\beta_2+(1-\beta_2)\ln(1-\beta_2)+\gamma_2\ln\gamma_2+(1-\gamma_2)\ln(1-\gamma_2) \\ &\quad +(8x-\alpha_1-\alpha_2-\beta_1-\beta_2-\gamma_1-\gamma_2-\delta_1)\ln(8x-\alpha_1-\alpha_2-\beta_1-\beta_2-\gamma_1-\gamma_2-\delta_1) \\ &\quad +(1-8x+\alpha_1+\alpha_2+\beta_1+\beta_2+\gamma_1+\gamma_2+\delta_1)\ln(1-8x+\alpha_1+\alpha_2+\beta_1+\beta_2 \\ &\qquad +\gamma_1+\gamma_2+\delta_1)\Big]. \end{aligned} \tag{4}$$

Applying Eq. (4) to deducing the free energy and the equilibrium equations based on the present formula concerning the 9 types above, the following equations will be obtained:

[O] Perfect disordered type

$$\alpha_1 = \alpha_2 = \cdots = \delta_2 = x.$$

$$f = 4(6+\mu)x^2+8\theta[x\ln x+(1-x)\ln(1-x)]. \tag{5}$$

[I_0] CuAu type

$$\alpha_1=\alpha_2=\beta_1=\beta_2\equiv\alpha,\quad \gamma_1=\gamma_2=\delta_1=\delta_2=2x-\alpha.$$

$$\begin{aligned} f = &-4[(2-\mu)(\alpha^2-2x\alpha)-2(2+\mu)x^2] \\ &+4\theta[\alpha\ln\alpha+(1-\alpha)\ln(1-\alpha)+(2x-\alpha)\ln(2x-\alpha)+(1-2x+\alpha)\ln(1-2x+\alpha)], \end{aligned} \tag{6}$$

$$(2-\mu)(\alpha-x) = \frac{\theta}{2}[\ln\alpha-\ln(1-\alpha)-\ln(2x-\alpha)+\ln(1-2x+\alpha)]. \tag{6'}$$

[I_1] Cu_3Au type

$$\alpha_1=\alpha_2\equiv\alpha,\quad \beta_1=\beta_2\equiv\beta,\quad \gamma_1=\gamma_2=\delta_1=\delta_2=\frac{1}{2}(4x-\alpha-\beta).$$

$$\begin{aligned} f = &-\frac{1}{2}[(2-\mu)(3\alpha^2+3\beta^2+2\alpha\beta-8x\alpha-8x\beta)-16(2+\mu)x^2] \\ &+2\theta\Big[\alpha\ln\alpha+\beta\ln\beta+(1-\alpha)\ln(1-\alpha)+(1-\beta)\ln(1-\beta)+(4x-\alpha-\beta)\ln(4x-\alpha-\beta) \\ &\quad +(2-4x+\alpha+\beta)\ln(2-4x+\alpha+\beta)-2\ln 2\Big], \end{aligned} \tag{7}$$

$$\begin{cases} (2-\mu)(3\alpha+\beta-4x) = 2\theta[\ln\alpha+\ln(2-4x+\alpha+\beta)-\ln(1-\alpha)-\ln(4x-\alpha-\beta)], \\ (2-\mu)(\alpha+3\beta-4x) = 2\theta[\ln\beta+\ln(2-4x+\alpha+\beta)-\ln(1-\beta)-\ln(4x-\alpha-\beta)]. \end{cases} \tag{7'}$$

[I_2] Cu_3Au type

$$\alpha_1=\alpha_2\equiv\alpha,\quad \beta_1=\beta_2=\gamma_1=\gamma_2=\delta_1=\delta_2=\frac{1}{3}(4x-\alpha).$$

$$\begin{aligned} f = &-\frac{4}{3}[(2-\mu)(\alpha^2-2x\alpha))-4(4+\mu)x^2] \\ &+2\theta[\alpha\ln\alpha+(1-\alpha)\ln(1-\alpha)+(4x-\alpha)\ln(4x-\alpha)+(3-4x+\alpha)\ln(3-4x+\alpha)], \end{aligned} \tag{8}$$

$$(2-\mu)(\alpha-x) = \frac{3}{4}\theta[\ln\alpha-\ln(3-4x+\alpha)-\ln(1-\alpha)-\ln(4x-\alpha)]. \tag{8'}$$

When $x=1/2$, $[I_0]$ is included in $[I_1]$, and $[I_2]$ above is a type conceivable only in the range of $1 \geqslant x \geqslant 1/4$.

$[II_0]$ CuPt type(†)

$$\alpha_1=\beta_1=\gamma_1=\delta_1\equiv a, \quad \alpha_2=\beta_2=\gamma_2=\delta_2=2x-a.$$

$$f = 24x^2+4\mu[a(2x-a)] + 4\theta[a\ln a+(1-a)\ln(1-a)+(2x-a)\ln(2x-a)+(1-2x+a)\ln(1-2x+a)], \quad (9)$$

$$2\mu(a-x)=\theta[\ln a+\ln(1-2x+a)-\ln(1-a)-\ln(2x-a)]. \quad (9')$$

$[II_1]$

$$\alpha_1=\beta_1=\gamma_1=\delta_1=a, \quad \alpha_2=b, \quad \beta_2=\gamma_2=\delta_2=\frac{1}{3}(8x-4a-b).$$

$$f=-\frac{2}{3}[(a+b)^2-4x(a+b)-32x^2]-4\mu[a^2-2x\,] + \theta\begin{Bmatrix}4a\ln a+b\ln b+4(1-a)\ln(1-a)+(1-b)\ln(1-b)+(8x-4a-b)\ln(8x-4a-b)\\ +(3-8x+4a+b)\ln(3-8x+4a+b)-3\ln 3\end{Bmatrix}, \quad (10)$$

$$\begin{cases}\frac{1}{3}[(a+b)-2x]+2\mu[a-x]=\theta[\ln a+\ln(3-8x+4a+b)-\ln(1-a)-\ln(8x-4a-b)],\\ \frac{4}{3}[(a+b)-2x]=\theta[\ln b+\ln(3-8x+4a+b)-\ln(1-b)-\ln(8x-4a-b)].\end{cases} \quad (10')$$

$[II_2]$

$$\alpha_1=\beta_1=\gamma_1=\delta_1\equiv a, \quad \alpha_2\equiv b, \quad \beta_2\equiv c, \quad \gamma_2=\delta_2=\frac{1}{2}(8x-4a-b-c).$$

$$f=-\frac{1}{4}[3(a+b)^2+3(a+c)^2+2(a+b)(a+c)-16x\{(a+b)+(a+c)\}-64x^2]-4\mu[a^2-2x\,] + \theta\begin{Bmatrix}4a\ln a+b\ln b+c\ln c+4(1-a)\ln(1-a)+(1-b)\ln(1-b)+(1-c)\ln(1-c)\\ +(8x-4a-b-c)\ln(8x-4a-b-c)+2(2-8x+4a+b+c)\ln(2-8x+4a+b+c)\\ -2\ln 2\end{Bmatrix}, \quad (11)$$

$$\begin{cases}\frac{1}{2}[2a+b+c-4x]+2\mu[a-x]\\ \qquad =\theta[\ln a+\ln(2-8x+4a+b+c)-\ln(1-a)-\ln(8x-4a-b-c)],\\ \frac{1}{2}[4a+3b+c-8x]=\theta[\ln b+\ln(2-8x+4a+b+c)-\ln(1-b)-\ln(8x-4a-b-c)],\\ \frac{1}{2}[4a+b+3c-8x]=\theta[\ln c+\ln(2-8x+4a+b+c)-\ln(1-c)-\ln(8x-4a-b-c)].\end{cases} \quad (11')$$

$[II_3]$

$$\alpha_1=\beta_1=\gamma_1=\delta_1\equiv a, \quad \alpha_2=\beta_2\equiv b, \quad \gamma_2\equiv c, \quad \delta_2=8x-4a-2b-c.$$

$$f=-[3(a+b)^2+(a+c)^2+2(a+b)(a+c)-8x(3a+2b+c)]-4\mu[a^2-2xa] + \theta\begin{Bmatrix}4a\ln a+2b\ln b+c\ln c+4(1-a)\ln(1-a)+2(1-b)\ln(1-b)+(1-c)\ln(1-c)\\ +(8x-4a-2b-c)\ln(8x-4\,.-2b-c)+(1-8x+4a+2b+c)\ln(1-8x+4a+2b+c)\end{Bmatrix}, \quad (12)$$

$$\begin{cases}[3a+2b+c-6x]+2\mu[a-x]\\ \qquad =\theta[\ln a+\ln(1-8x+4a+2b+c)-\ln(1-a)-\ln(8x-4a-2b-c)],\\ [4a+3b+c-8x]=\theta[\ln b+\ln(1-8x+4a+2b+c)-\ln(1-b)-\ln(8x-4a-2b-c)],\\ [4a+2b+2c-8x]=\theta[\ln c+\ln(1-8x+4a+2b+c)-\ln(1-c)-\ln(8x-4a-2b-c)].\end{cases} \quad (12')$$

(†) In a CuPt superlattice, the atomic ordering is identical with the antiferromagnetic spin order of the metal ions in antiferromagnet MnO etc.

[II$_4$]

$$\alpha_1=\beta_1=\gamma_1=\delta_1\equiv a,\quad \alpha_2=\beta_2=\gamma_2\equiv b,\quad \delta_2=8x-4a-3b.$$

$$f=-6[(a+b)^2-4x(a+b)]-4\mu[a^2-2xa]+\theta\begin{Bmatrix}4a\ln a+3b\ln b+4(1-a)\ln(1-a)+3(1-b)\ln(1-b)\\+(8x-4a-3b)\ln(8x-4a-3b)+(1-8x+4a+3b)\ln(1-8x+4a+3b)\end{Bmatrix},\tag{13}$$

$$\begin{cases}3[(a+b)-2x]+2\mu[a-x]=\theta[\ln a+\ln(1-8x+4a+3b)-\ln(1-a)-\ln(8x-4a-3b)],\\4[(a+b)-2x]\qquad\qquad=\theta[\ln b+\ln(1-8x+4a+3b)-\ln(1-b)-\ln(8x-4a-3b)].\end{cases}\tag{13'}$$

By solving numerically the above formulas and comparing the free energy of the different types, informations on the most stable state under finite temperature can be obtained.

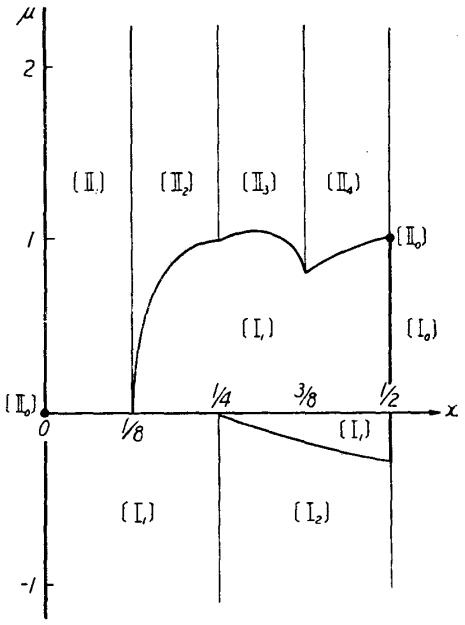

Fig. 2. Most stable state at 0°K. ($V>0$, $W\gtrless 0$)

3. Most stable stable state at absolute zero of temperature

The state of highest stability at 0°K can be obtained by comparing the energy terms (Table 1, 5th column) in the state of the highest degree of order of the respective type. The distribution of the most stable superlattice type versus the parameter μ and the concentration x is shown in Fig. 2. In Fig. 2, it will be seen that when μ, that is, the interaction between the second neighboring lattice, is small, the [I$_1$] or Cu_3Au type is the most stable in the vicinity of $x=1/4$, and that when μ increases and reaches the order of unity, the other types of $CuPt_7$, $CuPt_3$ and Cu_3Pt_5 become more stable.

III. The superlattice formation in Cu-Pt system

1. Experimental data

The equilibrium diagram of Cu-Pt system has been studied mainly by the measurement of electric resistance and X-ray analysis. The results may be summarized as follows:

1) Cu-Pt system is of a homogeneous solid solution and several types of superlattices have been found therein[6][7]. The phase diagram obtained by Schneider and Esch is shown in Fig. 3.

2) The superlattices found by the measurement of electrical resistance[7][8] and X-ray analysis are shown in Table 2.

3) The electrical resistance has been measured by Schneider-Esch[7] and more

(6) C. H. Johanson und I. O. Linde, Ann. Physik, **78** (1925), 439; **82** (1927), 449, 452.
(7) A. Schneider und V. Esch, Zeit. Elektrochem., **50** (1944), 290.
(8) S. Nagasaki, *Private communication.*

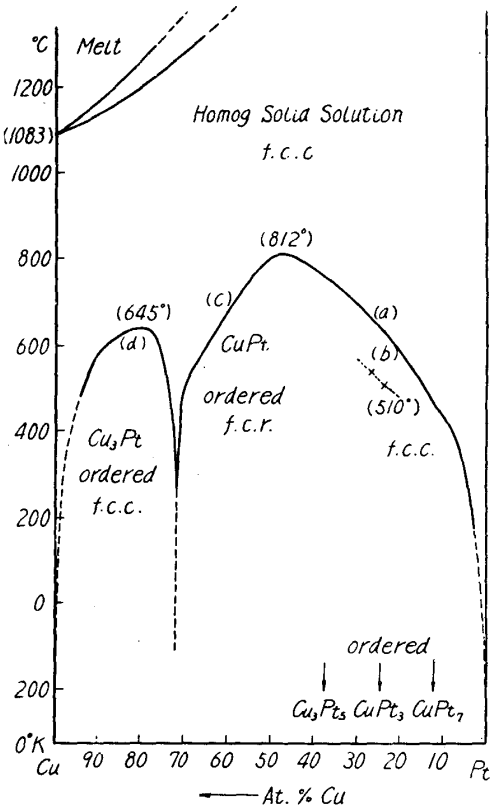

Fig. 3. Phase diagram of Cu–Pt system. (After Schneider u. Esch)

recently, by Nagasaki[8]. According to their results, at the concentrations near 25 per cent of Cu, a double-stepped change in electrical resistance was observable at 510°C and 642°C, which may be due probably to the double transitions of $CuPt_3 \rightarrow CuPt \rightarrow$disorder.

4) In the recent measurement of the specific heat of 25 per cent of Cu alloy by Nagasaki, two peaks of specific heat corresponding to the above two transition points were observed, showing the second order transitions of $CuPt_3 \rightarrow CuPt$ and $CuPt \rightarrow$ disorder, and the total heat absorption of about 240 cal/mol, the former being about 1/3 of the latter.

5) The measurement of the electro-osmotic pressure by Weidke and Matthes[9] showed that the configurational energy of order was 910 cal/mol (0.04 e.v. per atom) at the stoichiometric concentration.

6) According to the X-ray measurement of long range order by Walker[10], the transition of stoichiometric CuPt superlattice was of the first order.

Table 2. Superlattices in Cu–Pt alloy.

at.% Cu	Superlattice type[6][7]	Structure[6][7]	Max. transition temperature[7]
100~72%	$Cu_3Au(Cu_3Pt)$ $[I_1]$	*f. c. c.*	645°C (80%Cu)
72~ 0%	CuPt $[II_0]$	*f. c. r.* †	812°C (50%Cu)
※ 37%ca.	Cu_3Pt_5 (111) plane ordering $[II_n]$	*f. c. r.*	—
25%ca.	$CuPt_3$	↓	510°C (25%Cu)
13%ca.	$CuPt_7$	*f. c. c.*	498°C (13.5%Cu)

※ Schneider and Esch[7] could not find this type of superlattice.

† Rhombohedrality of CuPt superlattice is order of few minuets, hence it can be regarded almost *f. c. c.* (See refference (6) and (10))

2. Interpretation of the experimental results

(i) $P_i^{\nu}-T$ curve and specific heat

By solving numerically the equilibrium conditions (6′)-(13′) for the respective types of superlattices and comparing the values of free energies (5)-(13), $P_i^{\nu}-T$ curves would be obtained. It was deduced that $[II_n]$ types, ($n = 1, 2, 3, 4$), would appear at low temperature in the range below 50 per cent of Cu when μ is considerably large, while at high temperature the phase of CuPt $[II_0]$ type

(9) F. Weibke und H. Matthes, Zeit. Elektrochem., **47** (1941), 421.

(10) C. B. Walker, J. Appl. Phys., **23** (1952), 118.

would appear, and that when μ is comparatively small, Cu_3Au [I_1] type occurred. As an example of the former case, the $P_i^{\nu}-T$ curve of $CuPt_3$ solved with $\mu=1.5$ is shown in Fig. 4(A). On the other hand, the specific heat C_v might be calculated by dU/dT. The results showed double changes corresponding to each transition shown in Fig. 4(B). The orders of transition in the different types were also investigated, the results being shown in Table 3. When the values in this table and the results of the experiments given in 1. of this section are compared with one another, it should be conceded that the results are not satisfactory in respect of the order of transition, but it should be pointed out that there is some difficulty in expecting high accuracy in respect of the order of transition of this type within the limit of Bragg-Williams' approximation. In addition, if exact experimental determination of the order of transition is aimed at, it might be necessary to measure the specific heat and electrical resistance under the perfect thermal equilibrium state, which might be unexpected in the former experiments due to the high relaxation of the phase change in the alloys of transition metals.

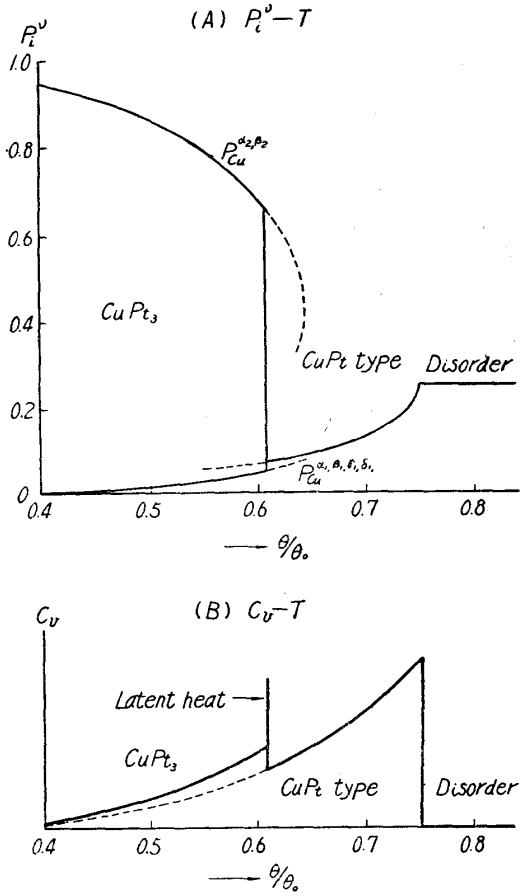

Fig. 4. $P_i^{\nu}-T$ and C_v-T curve for $\mu=1.5$ and $x=0.25$; θ_0 represents the critical temperature for $x=0.50$.

Table 3. Transitions.

Theory ($n=1,2,3,4$)		Experiment			
Transition	Order of transition		Method	Order	Transition heat
[I_1]→[O]	1st.	75%Cu [I_1]→[O]	Electrical resistance[7]	1st. ?	—
[II_0]→[O]	2nd.	50%Cu[II_0]→[O]	X-ray mesurement[10]	1st.	910 cal/mol[9]
		25%Cu[II_0]→[O] 〃	Specific heat[8] Electrical resistance[7]	2nd. 1st. ?	ca. 180 cal/mol[8]
[II_n]→[II_0]	1st	25%Cu[II_2]→[II_0] 〃	Specific heat[8] Electrical resistance[7]	2nd. 1st.	ca. 60 cal/mol[8]
[II_n]→[O]	1st.	12.5%Cu[II_1]→[O]	Electrical resistance[7]	1st.	—

(ii) Phase diagram

To derive the phase diagram by the aid of the theory developed above, the remarkable change in μ should be taken into consideration according as the change

of concentration. First, in the Pt-rich side within the range of $x < 0.5$, the value of μ does not so much vary with concentration, and the measured transition temperature versus concentration may be deduced by taking $\mu = 1.5 \sim 1.3$ (Fig. 5).

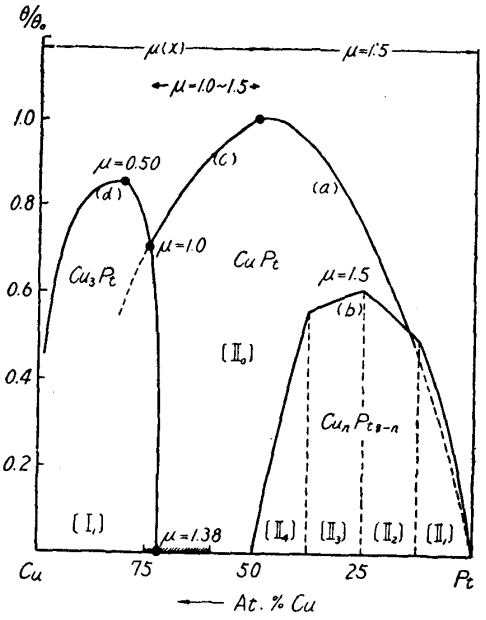

Fig. 5. Theoretical phase diagram of Cu–Pt system.

In these cases, as stated above, the superlattices of $CuPt_7$, $CuPt_3$ and Cu_3Pt_5 types are more stable than those of CuPt type, and so a transition from the former to the latter occurs in the *b*-curve shown in the Fig. 5. The transition temperature varies with the change of the value of μ, and the numerically values are shown in Table 4. On the other hand, in the Cu-rich side where $x > 0.5$, it must be postulated that the value of μ gradually diminishes with increase of x, in order to reproduce theoretically the phase diagram of experimental one. Thus, we should bear in mind that while the value of x rises from 0.5 to 0.76, the value of μ falls from 1.5 to 1.0, a transition of superlattice type (CuPt type→Cu_3Pt type) taking place at the latter point, and that with further rise of the value of x the value of μ tends to diminish continuously. Our theoretical phase diagram based on the above-mentioned change of μ value is given in Fig. 5.

Table 4. Variation of transition temperature with μ.

Value of θ_n/θ_0 { θ_n and θ_0 represent the transition temperatures of Cu_nPt_{8-n} $(n=1,2,3)$ and CuPt superlattices.

μ	$CuPt_7$	$CuPt_3$	Cu_3Pt_5
0.50	~1.2	Unstable	Unstable
1.00	0.676	~0.85	~0.85
1.25	0.564	~0.74	0.690
1.50	0.484	0.609	0.556
1.75	0.420	0.519	0.462
2.00	0.368	0.464	~0.4

It is to be noted that in the perfect thermal equilibrium state two-phase region must be found at the boundary of the regions of both superlattices, Cu_3Pt and CuPt, and that these two phases transform into a disordered state by eutectoid reaction. It can be concluded from a thermodynamical consideration that the boundary of such a two-phase region extends in the range of 60~75 per cent Cu at 0°K. It can be considered, however, that this kind of wide two-phase region has not been hitherto observed, because the specimens used in previous experiments were not in perfect thermal equilibrium. The theoretical phase diagram shown in Fig. 5 is one which excludes the removement of concentration by such a two-phase reaction.

By comparing the order-disorder transformation points plotted in this theoretical phase diagram with those of the experimental values, the absolute values of the nearest and the second neighbor interaction energies in Cu-Pt system, V and W, may be obtained as functions of the concentration. The values thus obtained of $V(x)$, $W(x)$ and $\mu(x)$ are shown in Fig. 6. The accuracy of these curves near both sides of Cu and Pt may be lost due to the fail of Bragg-Williams' approximation. It can be seen, however, that as the concentration changes, the relative magnitude of V and W is reversed both in Cu-rich and Pt-rich sides, indicating the appearance of two different types of superlattices, [I] and [II]. The physical interpretation of this finding will be stated in the next paragraph, and it may be pointed out here that in the above, we have succeeded in defining the change of the interaction energy between the neighbors accompanied by the change of concentration, for the purpose of explaining the phase diagram of Cu-Pt system.

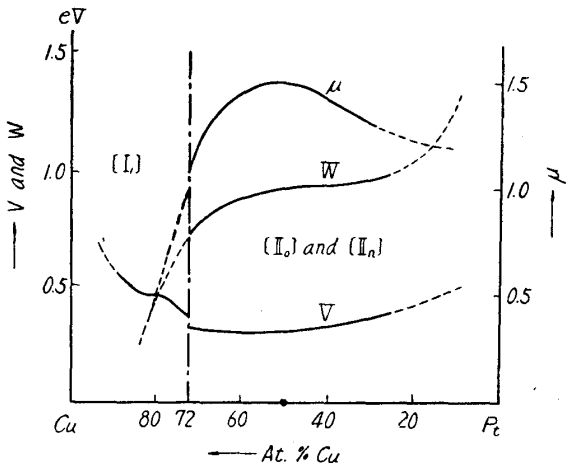

Fig. 6. Changes of V W and μ as a function of concentration.

IV. Discussions on ordering energy

The ordering energy of superlattices should be calculated exactly from the difference between the cohesive energies of the order and the disordered states of the alloy, but even the surest method now available for calculating the cohesive energy of metals and alloys—for example, the Celler method—are apt to accompany rather large errors. Besides, since the determination of the electronic structure of the alloy in disordered state is practically impossible, the ordering energy calculated by such a method will be within the limits of errors. So, in the following, some discussions will only be given for the various factors that would influence the difference between the energies of the ordered and the disordered states.

First, the ordering energy of the superlattice CuPt in the stoichiometric concentration will be deduced by applying Mott's method, and then the changes of ordering energies due to the change in concentration will be explained by attributing them to the increase of *s*-electrons caused by adding Pt to Cu. Since, in the superlattice of CuPt, the nearest neighbors of any lattice point are occupied by an equal number (six) of Cu and Pt atoms, the numbers of the like and the unlike atoms being equal to those of the disordered state. Therefore, it may be assumed that the nearest neighbor interaction contributes nothing to the formation of CuPt superlattice(but not for Cu_nPt_{8-n} superlattices). On the other hand, since the second neighbors consist of six unlike atoms but not like atoms, it may be presumed that only the ordering energy W of the second neighbors contributes to the formation

of such a superlattice. As no term caused by exchange repulsion of ion cores significant only among nearest neighbor atoms comes into W, the above-mentioned screened electrostatic interaction will be of importance.

According to Mott, the potential $\Phi(r)$ around the atoms has been calculated by solving the Thomas-Fermi equation, $\nabla^2\Phi(r)=q^2\Phi(r)$, under the boundary condition required between the second neighbor atoms. Then, estimating the charge ε with a sphere of radius half the lattice constant a, it will be obtained

$$\varepsilon = \frac{1}{4\pi}\oint\frac{\partial\Phi}{\partial n}\,dS = \pm\frac{eq(a/2)}{\sinh\{q(a/2)\}}, \tag{14}$$

where e is the charge of electron and q the screening constant given by $q = 2m^{*\frac{1}{2}}e(3N_0/\pi)^{\frac{1}{6}}\hbar^{-1}$ (where N_0 is the concentration of screening electron and m^* the effective mass of electrons). As the CuPt superlattice may be considered to be the interpenetration of four ionic crystals of NaCl type, the electro-static energy W_{theo} may be represented, using this ε, in the form of

$$W_{theo} = \frac{1}{2}\frac{\alpha_M}{a}\varepsilon^2\times 4. \tag{15}$$

Here, $\alpha_M=1.748$ is the Madelung constant for NaCl type.

Now, some experimental facts concerning such alloys will be estimated.

(1) The ordering energy can be estimated by using the maximum order-disorder transition temperature ($T_c = 1085$°K) derived from phase diagram (Fig. 3); the value of W_{exp} will be obtained by means of the ordering energy and transition temperature relation as follows:

$$W_{exp} = \frac{2}{3}kT_c = 0.062 \text{ e. v.} \tag{16}$$

(2) Ordering energy is also obtained from the measured values of the electro-osmotic pressure by the method of Weibke and Matthes:

$$W_{exp} = 0.04 \text{ e. v.} \tag{16'}$$

Therefore, the value of W is of the order of 0.04~0.06 e. v.

By calculating the screening constant q which is consistent with the value W (14) and (15), $q = 3.4\sim3.5\times10^8\text{cm}^{-1}$, or $1/q = 0.294\sim0.286\times10^{-8}$cm, which approximately agrees with $1/q\simeq0.3\times10^{-8}$cm estimated by Mott[11] from the increase of electric resistance when a small quantity of divalent metal is dissolved in monovalent metal. This value can be approximately accounted for, if the number N_0 of the s-electron, or the conductive electron of CuPt in above explicit equation of q, is taken to be half that of Cu and if their effective mass m^* is about $4m$.

Next, as shown in Fig. 6, the change of the ratio μ between V and W with concentration can be explained from the structure of energy band of this alloy(**) as follows: As, in the Pt-rich side, the electrons in the d-band of alloys are

(11) N. F. Mott and H. Jones "*The Theory of the Properties of Metals and Alloys*", (Oxford Univ. Press. New York), (1936), p. 292.

(**) The s and d bands of this alloy are tentatively assumed to retain the properties of $4s$ and $3d$ bands in Cu and of $6s$ and $5d$ bands in Pt. For exact determination, the electronic structure of these superlattices must first be studied.

increased by replacing the Pt atom with Cu, the number of the electrons in the *s*-band of this alloy will undergo little change. Consequently, the above screening constant also will remain unchanged within the range of $\mu = 1.5 \sim 1.3$. When the Cu content reaches about 50 per cent, the above *d*-band will be completely filled up, and so a further addition of Cu as solid solution will cause a rapid increase of *s*-electrons and of the value of V, resulting in an equally rapid diminution of W, and the superlattice makes the transition from the type [II] to [I] at $x=0.72$. When the Cu content rises further and the transition to the type [I] or Cu_3Pt type is completed, the energy term due to the exchange repulsion of the ion cores in V becomes markedly effective, and so V increases in value.

Summary

(1) Superlattices of many types appeared in the alloys of Cu-Pt system according as the change of the relative concentrations of the component metals.

(2) This phenomenon was inferred to be due to the rather large value of the second neighbor interaction and to the change of this value accompanied by the increase of *s*-electrons due to the addition of Cu.

This investigation was supported by the Scientific Research Fund granted by the Ministry Education.